Modulation instability induced by cross-phase modulation in optical fibers

Govind P. Agrawal*
AT&T Bell Laboratories, Murray Hill, New Jersey 07974

P. L. Baldeck and R. R. Alfano
Institute for Ultrafast Spectroscopy and Photonics Application Laboratory, Electrical Engineering and Physics Departments, The City College of New York, New York, New York 10031

(Received 22 September 1988)

When two optical beams copropagate inside a single-mode fiber, the intensity-dependent refractive index couples the two beams through a nonlinear phenomenon known as cross-phase modulation (XPM). Such an XPM-induced interaction between the two waves can destabilize the steady state and lead to temporal modulations (self-pulsing) in the presence of group-velocity dispersion. This phenomenon is analogous to the modulation instability of a single beam occurring in the anomalous-dispersion regime of the fiber. The XPM-induced modulation instability can occur even in the normal-dispersion regime. The features of XPM-induced modulation instability are discussed in detail. This phenomenon may be useful for generating ultrashort pulses (< 100 fs) in the visible region of the optical spectrum.

I. INTRODUCTION

Many nonlinear physical systems exhibit an instability that leads to a self-induced modulation of the steady state as a result of an interplay between the nonlinear and dispersive effects. This phenomenon is referred to as the modulation instability and has been studied in such diverse fields as fluid dynamics,[1,2] nonlinear optics,[3–5] and plasma physics.[6–9] In the context of optical fibers, modulation instability requires anomalous group-velocity dispersion (GVD) and manifests itself as breakup of continuous-wave (cw) or quasi-cw radiation into a train of ultrashort pulses. It has been extensively studied[9–23] because of its fundamental nature as well as technological applications. The physical mechanism behind modulation instability is self-phase modulation (SPM) that leads to self-amplitude modulation in the presence of anomalous GVD. Although the observation of modulation instability in optical fibers by using cw beams is hampered by the competing nonlinear effects (such as stimulated Brillouin scattering), it has recently been observed under quasi-cw condition.[14,15] These experiments were performed in the infrared region beyond 1.3 μm in order to operate in the anomalous-GVD regime of the silica fiber.

It was recently predicted by Agrawal[24] that a new kind of modulation instability can occur even in the normal-GVD regime when two or more optical fields copropagate inside the fiber. The physical mechanism behind this novel phenomenon is cross-phase modulation (XPM) which refers to the nonlinear phase change of an optical field induced by other copropagating fields.[25–33] The XPM-induced modulation instability has been observed in an experiment[34] where the second copropagating field was generated internally through stimulated Raman scattering. An experiment in which both waves were incident externally at the fiber input has also been reported.[35]

The objective of this paper is to extend the theory of XPM-induced modulation instability given in Ref. 24. There, the modulation frequencies associated with the two cw waves were assumed to be the same. This need not be the case in general, as also indicated by our experimental data.[34] A linear-stability analysis of the coupled-amplitude equations is carried out in this paper by allowing the perturbation frequencies to be different for each wave. The paper is organized as follows. Starting from Maxwell's wave equation, we derive the coupled-amplitude equations for the slowly varying envelopes of the two beams. These equations are readily solved to obtain the steady-state solution in the case of cw beams. The stability of the steady state is examined in Sec. III where we carry out a linear-stability analysis. This provides us with a modulation-instability condition. The gain and the frequencies associated with the modulation instability are discussed in Sec. IV for the four cases in which either the beam 1 or 2 or both beams propagate in the normal or anomalous GVD regimes of the fiber. The results are discussed and summarized in Sec. V.

II. COUPLED-AMPLITUDE EQUATIONS

We consider the case in which two optical beams are incident on single-mode, polarization-preserving fiber. Both beams are assumed to be linearly polarized along one of the principle axes of the fiber. The wave-propagation problem is then considerably simplified since it can be solved by using the scalar wave equation

$$\nabla^2 E - \frac{1}{c^2}\frac{\partial^2}{\partial t^2}(\bar{n}^2 E) = 0 , \tag{1}$$

where E is the total electric field, c is the velocity of light in vacuum, and the refractive index $\bar{n}$ is given by

$$\bar{n} = n(\omega) + n_2 |E|^2 . \tag{2}$$

The frequency dependence of the linear part $n(\omega)$ results from GVD in optical fibers. The fiber nonlinearity is included through the nonlinear-index coefficient n_2 in Eq. (2). The frequency dependence of n_2 can generally be ignored. For silica fibers $n_2 \simeq 3.2\times10^{-20}$ m^2/W.

The total electric field E can be written in the form

$$E(x,y,z,t)=F(x,y)\sum_{j=1}^{2}A_j(z,t)\exp[i(k_jz-\omega_jt)]\ , \tag{3}$$

where ω_j is the optical frequency, $k_j=n_j\omega_j/c$ with $n_j=n(\omega_j)$, A_j is the amplitude assumed to be slowly varying both with z and t, and $F(x,y)$ is the transverse distribution of the fundamental fiber mode. By substituting Eq. (3) in Eq. (1) and expending k_j in a Taylor series around ω_j, the amplitudes A_i and A_2 are found to satisfy the following two coupled-amplitude equations:

$$\frac{\partial A_1}{\partial z}+\frac{1}{v_{g1}}\frac{\partial A_1}{\partial t}+\frac{i}{2}\beta_1\frac{\partial^2A_1}{\partial t^2} =i\gamma_1(|A_1|^2+2|A_2|^2)A_1\ , \tag{4}$$

$$\frac{\partial A_2}{\partial z}+\frac{1}{v_{g2}}\frac{\partial A_2}{\partial t}+\frac{i}{2}\beta_2\frac{\partial^2A_2}{\partial t^2} =i\gamma_2(|A_2|^2+2|A_1|^2)A_2\ , \tag{5}$$

where the group velocity

$$v_{gj}=\left[\frac{dk_j}{d\omega}\right]^{-1}_{\omega=\omega_j}\quad(j=1,2), \tag{6}$$

the GVD coefficient

$$\beta_j=\left[\frac{d^2k_j}{d\omega^2}\right]_{\omega=\omega_j}\ , \tag{7}$$

and the nonlinear coefficient

$$\gamma_j=n_2\omega_j/(cA_{\text{eff}})\ . \tag{8}$$

The effective core area in Eq. (8) is defined by

$$A_{\text{eff}}=\frac{\left[\int\int|F(x,y)|^2dx\,dy\right]^2}{\int\int|F(x,y)|^4dx\,dy}\ , \tag{9}$$

where the integrals extend over the entire transverse range. $F(x,y)$ in Eq. (9) is the field distribution associated with the HE_{11} mode. The integrals in Eq. (9) can be evaluated by using the modal distribution or its Gaussian approximation.[23] Typically A_{eff} is somewhat larger than the fiber-core area. Strictly speaking, Eqs. (4) and (5) apply to a polarization-preserving fiber. However, the modulation-instability experiments[14,15] indicate that the results can be applied even to fibers in which the input polarization is not preserved during propagation inside the fiber.

In obtaining Eqs. (4) and (5) we neglected the terms of the form $A_1^2A_2^*$. These terms are responsible for four-wave mixing and do not contribute significantly unless the phase-matching condition is satisfied; we assume that phase matching does not occur. We have also neglected the fiber loss. This is not a limitation since typical fiber lengths used in the experiment[33–35] are smaller than the absorption length α^{-1}. The fiber loss can be included by adding a term αA_j on the left-hand side of Eqs. (4) and (5). The two terms on the right-hand side of these equations are responsible for SPM and XPM, respectively. Note the factor of 2 in front of the XPM term. It is the XPM-induced coupling between the two waves that is responsible for modulation instability in the normal-GVD regime.

Equations (4) and (5) describe the evolution of two copropagating optical pulses with nonoverlapping spectra inside an optical fiber. The XPM-induced interaction between the two pulses can lead to novel spectral and temporal changes[25–32] whose investigation often requires a numerical approach. For the discussion of modulation instability, however, we need only the steady-state solution of Eqs. (4) and (5). Under cw or quasi-cw conditions, the time derivatives in these equations can be ignored. The resulting analytic solution is given by

$$\overline{A}_j(z)=\sqrt{P_j}\exp(i\phi_j)\ , \tag{10}$$

where $j=1$ or 2, P_j is the incident optical power, and the phase

$$\phi_j(z)=\gamma_j(P_j+2P_{3-j})z\ . \tag{11}$$

Equations (10) and (11) show that the two cw beams would propagate through the optical fiber unaffected except for acquiring a phase shift which increases linearly with distance and depends on the powers of both beams. Further, the phase shifts are different for the two beams if their powers are different. Before reaching this conclusion, however, one must ask whether the steady-state solution (10) is stable against small perturbations. We answer this question in the next section by performing a linear-stability analysis of the steady-state solution.

III. LINEAR-STABILITY ANALYSIS

The stability of the steady state is examined by considering how weak, time-dependent perturbations evolve along the fiber. More specifically, if such perturbations grow exponentially, the steady state is unstable. In the linear-stability analysis, the perturbed amplitude is of the form

$$A_j(z,t)=[\sqrt{P_j}+a_j(z,t)]\exp(i\phi_j)\ , \tag{12}$$

where $|a_j|^2\ll P_j$. If we substitute Eq. (12) in Eqs. (4) and (5) and neglect the quadratic and higher-order terms in a_j, the perturbations a_1,a_2 are found to satisfy the following linearized set of two coupled equations:

$$\frac{\partial a_1}{\partial z}+\frac{1}{v_{g1}}\frac{\partial a_1}{\partial t}+\frac{i}{2}\beta_1\frac{\partial^2a_1}{\partial t^2} =i\gamma_1P_1(a_1+a_1^*)+2i\gamma_1(P_1P_2)^{1/2}(a_2+a_2^*)\ , \tag{13}$$

$$\frac{\partial a_2}{\partial z}+\frac{1}{v_{g2}}\frac{\partial a_2}{\partial t}+\frac{i}{2}\beta_2\frac{\partial^2a_2}{\partial t^2} =i\gamma_2P_2(a_2+a_2^*)+2i\gamma_2(P_1P_2)^{1/2}(a_1+a_1^*)\ . \tag{14}$$

The last term these equations is due to XPM and vanishes if only one beam is incident at the fiber.

Equations (13) and (14) can be easily solved because of their linear nature. We assume a general solution of the form

$$A_j = U_j \cos[Kz - \Omega_j(t - z/v_{gj})] + iV_j \sin[Kz - \Omega_j(t - z/v_{gj})] , \quad (15)$$

where $j = 1$ or 2, Ω_j is the frequency of perturbation, and K is the wave number. For a perturbation moving with the group velocity v_{gj}, the effective wave number $K_j = K + \Omega_j / v_{gj}$. The substitution of Eq. (15) in Eqs. (13) and (14) provides a set of four homogeneous equations for U_1, U_2, V_1, and V_2. This set has a nontrivial solution only if the determinant of the coefficient matrix vanishes. By expanding the determinant, we obtain the following dispersion relation:

$$(K^2 - h_1)(K^2 - h_2) = C^2 , \quad (16)$$

where

$$h_j = \tfrac{1}{4}\beta_j^2 \Omega_j^2 [\Omega_j^2 + \mathrm{sgn}(\beta_j)\Omega_{cj}^2] , \quad (17)$$

$$C = 2\Omega_1 \Omega_2 (\beta_1 \beta_2 \gamma_1 \gamma_2 P_1 P_2)^{1/2} , \quad (18)$$

and we have defined a characteristic frequency Ω_{cj} associate with each beam by using the relation

$$\Omega_{cj}^2 = 4\gamma_j P_j / |\beta_j| . \quad (19)$$

The dispersion relation provides a quadratic algebric equation in K^2 whose solution is

$$K^2 = \tfrac{1}{2}\{(h_1 + h_2) \pm [(h_1 + h_2)^2 + 4(C^2 - h_1 h_2)]^{1/2}\} . \quad (20)$$

The stability of the steady state is governed by Eq. (20). If the wave number K has an imaginary part, the perturbation grows exponentially, as is evident from Eq. (15). This unstable growth of weak perturbations is referred to as the modulation instability since is implies that the stable state of the system is a modulated state. In the literature on quantum optics such instabilities are often called self-pulsing instabilities for the same reason.[36,37] The necessary condition for modulation instability to occur from Eq. (20) is

$$h_1 h_2 < C^2 , \quad (21)$$

since K^2 then becomes negative resulting in a purely imaginary value of K.

The modulation-instability condition (21) can be written in a more transparent form by using Eqs. (17) and (18). The result is

$$[f_1^2 + \mathrm{sgn}(\beta_1)][f_2^2 + \mathrm{sgn}(\beta_2)] < 4 , \quad (22)$$

where f_1 and f_2 are the normalized modulation frequencies defined by

$$f_j = \Omega_j / \Omega_{cj} . \quad (23)$$

Equation (22) is the main result of this section. It shows that modulation-instability condition depends on the signs of the GVD coefficients β_1 and β_2. Both of them can be positive or negative depending on whether the wavelengths λ_1 and λ_2 ($\lambda_j = 2\pi c/\omega_j$) are shorter or longer than the zero-dispersion wavelength λ_D of the fiber. For silica fibers typically $\lambda_D \simeq 1.3$ μm, although it can be tailored to be in the range 1.3–1.6 μm through design modifications in the so-called dispersion-shifted fibers.[38]

In Sec. IV we consider the implications of the modulation-instability condition (22). Before considering the general case, it is instructive to discuss briefly the features of single-beam modulation instability. If only beam 1 is incident, $P_2 = 0$, and from Eq. (18), $C = 0$. Equation (16) then yields the dispersion relation $K^2 = h_1$. Modulation instability occurs if K^2 is negative or $h_1 < 0$. The necessary condition for this to occur is obtained from Eq. (17) and is given by

$$f_1^2 + \mathrm{sgn}(\beta_1) < 0 . \quad (24)$$

This condition should be compared with Eq. (22). The most notable aspect of Eq. (24) is that modulation instability cannot occur unless $\beta_1 < 0$, or the input beam is launched with a wavelength $\lambda_1 > \lambda_D$ to propagate in the anomalous-GVD regime. When $\beta_1 < 0$, the gain spectrum of the modulation instability is obtained by using

$$g = 2\,\mathrm{Im}(K) = |\beta_1 \Omega_1| (\Omega_{c1}^2 - \Omega_1^2)^{1/2} . \quad (25)$$

This is a well-known result.[15] It shows that fluctuations at frequencies $\Omega_1 \le \Omega_{c1}$ are amplified as a result of modulation instability and their power grows as $\exp(gz)$ along the fiber length. If we use Eq. (23), the gain can be written in terms of the normalized frequency f_1 as

$$g = (4\gamma_1 P_1) f_1 (1 - f_1^2)^{1/2} . \quad (26)$$

The gain is maximum for $f_1 = 1/\sqrt{2}$, and the maximum value is given by $g_{\max} = 2\gamma_1 P_1$. Note that the maximum gain does not depend on the GVD coefficient.

How does the modulation instability manifest in practice? If a perturbation is imposed externally by sending a weak probe together with the strong-cw beam at a frequency $\omega_1 + \Omega_1$, the perturbation would grow along the fiber with the gain given by Eq. (26). The situation is analogous to the four-wave-mixing configuration. In fact, modulation instability can be interpreted as a colinear four-wave mixing process phase matched by SPM. In this interpretation, two photons of frequency ω_1 are annihilated to create two different photons at the frequencies $\omega_1 + \Omega_1$ and $\omega_1 - \Omega_1$. Thus, not only the probe would be amplified by the modulation-instability gain, but at the same time a new wave at $\omega_1 - \Omega_1$ would be generated. The case in which a perturbation is imposed externally is referred to as induced modulation instability.[10,15]

Modulation instability can also occur spontaneously. In this case quantum noise serves as a weak perturbation imposed on the steady state. In general, spontaneous noise at all frequencies such that $\omega = \omega_1 + \Omega_1$ with $|\Omega_1| < \Omega_{c1}$ is amplified but different frequency components are amplified by different amounts. The frequency component corresponding to the maximum value of the gain becomes most intense. Such a selective growth of vacuum noise manifests as spontaneous generation of

two side bands located at $\omega_1 \pm \Omega_1$ in the optical spectrum centered at ω_1. The frequency Ω_1 is obtained by using $f_1 = 1/\sqrt{2}$ in Eq. (23). The use of Eq. (19) then gives the following expression for the modulation frequency:

$$\Omega_1 = (2\gamma_1 P_1/|\beta_1|)^{1/2} . \tag{27}$$

IV. XPM-INDUCED MODULATION INSTABILITY

The gain associated with the XPM-induced modulation instability is obtained from Eq. (20) by using the definition $g = 2\,\mathrm{Im}(K)$, where the factor of 2 implies that g is the power gain. Using the modulation-instability condition (21), together with the choice of the minus sign in Eq. (20), we obtain

$$g = \sqrt{2}\{[(h_1 - h_2)^2 + 4C^2]^{1/2} - (h_1 + h_2)\}^{1/2} , \tag{28}$$

where h_j ($j = 1$ or 2) is given by Eq. (17). By using Eqs. (19) and (23), h_j can be expressed in the form

$$h_j = 4\gamma_j^2 P_j^2 f_j^2 [f_j^2 + \mathrm{sgn}(\beta_j)] , \tag{29}$$

where the normalized modulation frequency $f_j = \Omega_j/\Omega_{cj}$ and Ω_{cj} is given by Eq. (19). Modulation instability occurs only when f_1 and f_2 satisfy the condition [see Eq. (22)]

$$[f_1^2 + \mathrm{sgn}(\beta_1)][f_2^2 + \mathrm{sgn}(\beta_2)] < 4 . \tag{30}$$

Equation (30) provides the domain of modulation instability in the f_1-f_2 plane. There are four cases of practical interest depending on whether none, one, or both beams propagate in the normal-GVD regime of the optical fiber. These cases are governed by the four possible combinations of the signs of β_1 and β_2 in Eq. (30). Figure 1 shows the modulation-instability domains for the four cases. In each case modulation instability can occur only for frequencies f_1 and f_2 lying below the curve that marks the boundary of the instability domain. Only one quadrant in which both f_1 and f_2 are positive is shown in Fig. 1. The most notable feature is that modulation instability can occur even when both beams propagate in the normal-GVD regime of the fiber. This case is of particular importance since each beam is stable against small perturbations in the absence of the XPM-induced coupling between the two beams.

How does the XPM-induced modulation instability manifest itself? Similar to the case of single beam modulation instability, each beam develops modulation sidebands in its spectrum separated from the center line at ω_j by the modulation frequency $\Omega_j = f_j \Omega_{cj}$ ($j = 1$ or 2). In the time domain, the beams develop temporal oscillations (or self-pulsing) at these modulation frequencies. The amplitude of the modulation sidebands or the temporal oscillations depends on the fiber length and the amount of gain given by Eq. (28). The modulation frequencies f_1 and f_2 depend on whether the modulation sidebands grow from vacuum noise or from an external perturbation imposed on the beams. Three cases are possible. First, both beams may be launched with a weak perturbation imposed on them. If the frequencies f_1 and f_2 of the perturbation lie within the modulation-instability domain of Fig. 1, the perturbation grows exponentially as $\exp(gz)$, where g is determined by Eq. (28). Second, an external perturbation may be imposed on only one beam. Then, the modulation frequency of the other beam corresponds to one that maximizes the gain g. Third, none of the beams has an external perturbation imposed on it. In that case f_1 and f_2 are determined by the requirement that g be maximum for both beams since those noise-frequency components experience maximum growth. Mathematically, we set

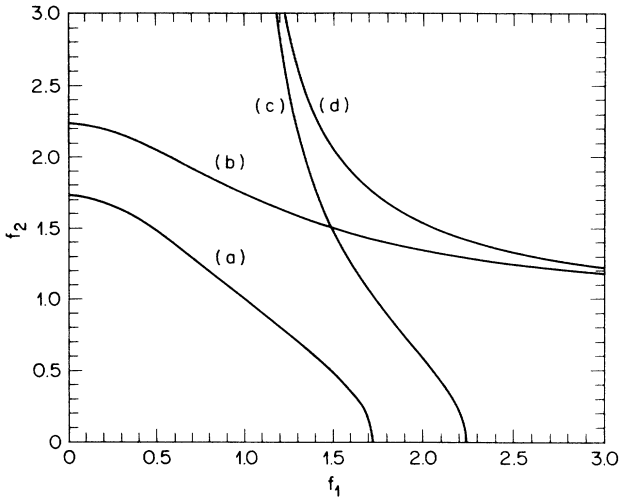

FIG. 1. Domains of modulation instability in the four cases of practical interest: (a) normal GVD for both beams ($\beta_1 > 0$, $\beta_2 > 0$), (b) normal GVD for beam 1 and anomalous GVD for beam 2 ($\beta_1 > 0$, $\beta_2 < 0$), (c) anomalous GVD for beam 1 and normal GVD for beam 2 ($\beta_1 < 0$, $\beta_2 > 0$) and (d) anomalous GVD for both beams ($\beta_1 < 0$, $\beta_2 < 0$). In each case modulation instability occurs only for normalized frequencies f_1 and f_2 lying below the curve.

$$\frac{\partial g}{\partial f_1} = 0 \text{ and } \frac{\partial g}{\partial f_2} = 0 . \tag{31}$$

We then obtain two algebraic equations for f_1 and f_2 whose solution satisfying the inequality

$$\frac{\partial^2 g}{\partial f_1^2}\frac{\partial^2 g}{\partial f_2^2} < \left[\frac{\partial^2 g}{\partial f_1 \partial f_2}\right]^2 \tag{32}$$

determines the frequencies f_1 and f_2. The maximum gain can then be obtained by using these values in Eq. (28). In the following we discuss the modulation frequencies and the gain for the four cases shown in Fig. 1.

Case (a): $\beta_1 > 0$, $\beta_2 > 0$. As mentioned earlier, this case is of particular importance since modulation instability does not normally occur in the normal-GVD regime of the optical fiber. Equations (28)–(30) with the choice of positive values of β_1 and β_2 determine both the modulation frequencies and the gain g. Figure 2 shows the variation of g with f_1 for several values of f_2 for the case $\gamma_1 P_1 = \gamma_2 P_2 = 2\ \mathrm{m}^{-1}$. Typically $\gamma_j = 0.01$–$0.03\ \mathrm{W}^{-1}$ in the visible and near-infrared regions for a single-mode fiber of core diameter 4–6 μm [see Eq. (8)]. Thus, the re-

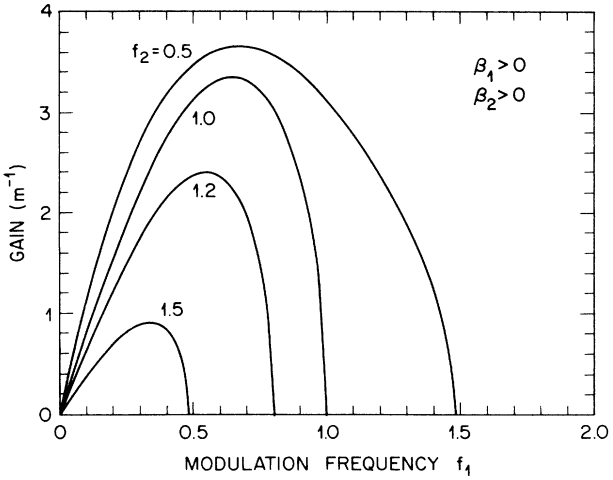

FIG. 2. Variation of gain with normalized modulation frequency f_1 for several values of f_2. Both beams experience normal GVD and their peak powers are such that $\gamma_1 P_1 = \gamma_2 P_2 = 2$ m^{-1}.

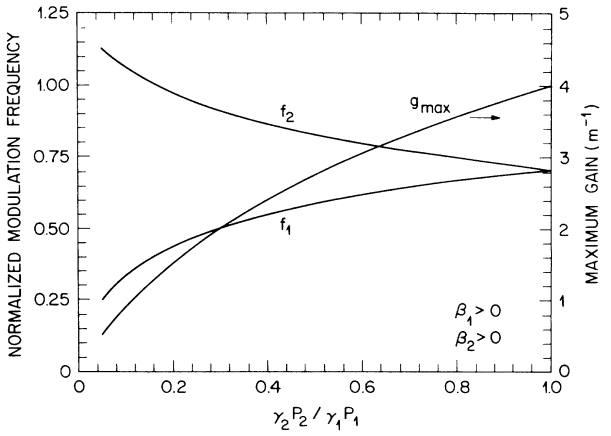

FIG. 3. Variation of the normalized modulation frequencies f_1 and f_2 with $\gamma_2 P_2/\gamma_1 P_1$ for $\gamma_1 P_1 = 2$ m^{-1} in the case of spontaneous modulation instability. The maximum gain is also shown. Even though f_2 increases with a reduction in P_2, $\Omega_2 = f_2 \Omega_{c2}$ actually decreases and becomes zero for $P_2 = 0$. Both beams experience normal GVD ($\beta_1 > 0, \beta_2 > 0$).

sults of Fig. 2 correspond to a power level ~ 100 W for each beam. It is not necessary to specify β_1 and β_2. Their values set a frequency scale used to normalize the modulation frequencies. If we use $\beta_j = 0.06$ ps^2/m and $\gamma_j P_j = 2$ m^{-1} in Eq. (19), $\Omega_{cj}/2\pi \simeq 2$ THz for $j = 1$ and 2. Thus, the actual modulation frequencies can be obtained by multiplying f_1 and f_2 by a number ~ 2 THz depending on the exact values of β_1 and β_2.

Figure 2 shows that for a fixed f_2, the gain is maximum at a value of f_1 that decreases with an increase in f_2. If the beam 2 is externally modulated at a frequency f_2, the beam 1 would develop modulation at a frequency f_1 corresponding to the peak value of the gain. This can be referred to as induced modulation instability since the modulation of beam 1 is induced by the external modulation of beam 2.

Spontaneous modulation instability refers to the case in which the beams develop modulation by themselves as they propagate inside the fiber. The modulation frequencies f_1 and f_2 are then determined by maximizing g with respect to both f_1 and f_2, as indicated by Eq. (31). Figure 3 shows f_1, f_2, and g_{max} as a function of the ratio $\gamma_2 P_2/\gamma_1 P_1$ for $\gamma_1 P_1 = 2$ m^{-1}. Noting that $\gamma_2/\gamma_1 = \lambda_1/\lambda_2$, where $\lambda_j = 2\pi c/\omega_j$, the abscissa corresponds roughly to the power ratio if the wavelengths of the two beams are close to each other. As one would expect, g_{max} decreases with a decrease in P_2/P_1. The modulation frequencies f_1 and f_2 change with P_2/P_1. Note, however, that the scaling factor Ω_{cj} also changes with the powers as $P_j^{1/2}$ for $j = 1$ or 2 [see Eq. (19)]. In fact, $\Omega_j = f_j \Omega_{cj}$ is nearly the same for both beams if $\beta_1 \simeq \beta_2$.

Case (b): $\beta_1 > 0, \beta_2 < 0$. In this case the beam 1 experiences normal GVD while the beam 2 propagates in the anomalous-GVD regime of the optical fiber. Figure 4 shows the gain curves for the case of induced modulation instability by assuming that the beam 2 has a weak modulation at the frequency f_2 imposed on it. All parameter values are identical to those used for case (a). The beam 1 develops modulation at the frequency f_1 corresponding to the peak of the gain curves in Fig. 4. When compared with case (a) shown in Fig. 2, the main difference is that the peak gain is larger by about a factor of 2. The modulation frequencies f_1 and f_2 are also generally larger. As seen in Fig. 1, f_2 can be quite large (~ 10 or more) and still the beam 2 can induce modulation on beam 1. These differences can be attributed to the anomalous GVD experienced by the beam 2.

The modulation frequencies f_1 and f_2 and the maximum gain g_{max} for the case of spontaneous modulation instability are shown in Fig. 5. This figure should be

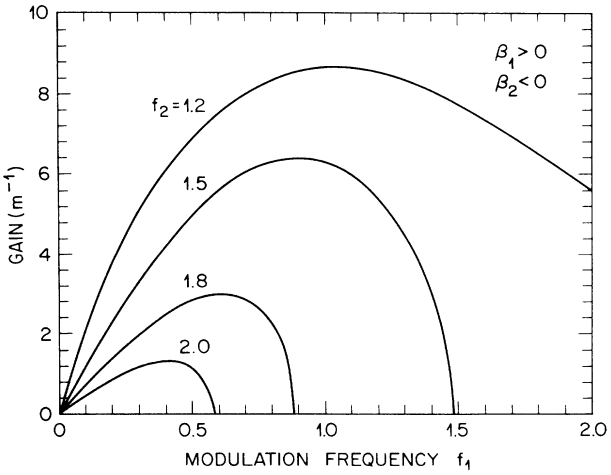

FIG. 4. Same as Fig. 2 except that beam 1 experiences normal GVD ($\beta_1 > 0$) while beam 2 experiences anomalous GVD ($\beta_2 < 0$).

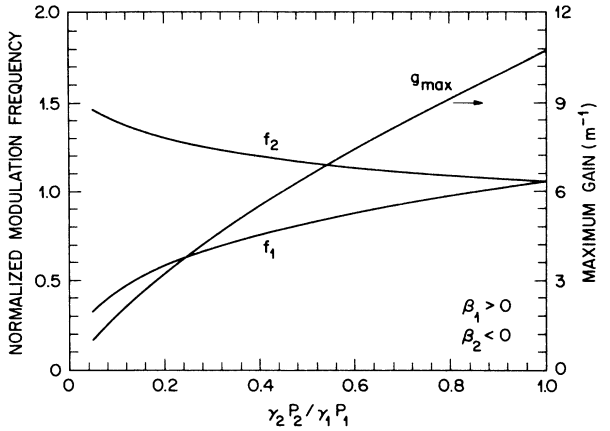

FIG. 5. Same as Fig. 3 except that beam 1 experiences normal GVD ($\beta_1 > 0$) while beam 2 experiences anomalous GVD ($\beta_2 < 0$).

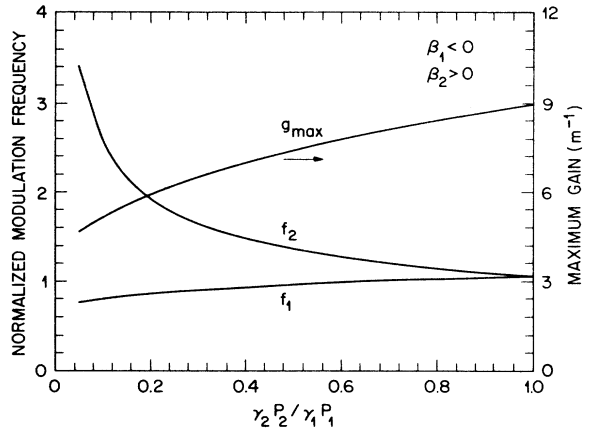

FIG. 7. Same as Fig. 3 except that beam 1 experiences anomalous GVD ($\beta_1 < 0$) while beam 2 experiences normal GVD ($\beta_2 > 0$).

compared with Fig. 3 to see the differences resulting from the propagation of beam 2 in the anomalous-GVD regime. Both g_{max} and f_j ($j = 1$ or 2) are larger in case (b) compared with case (a) but the qualitative behavior is the same.

Case (c): $\beta_1 < 0$, $\beta_2 > 0$. This case is complimentary to case (b) in the sense that the beam 1 now experiences anomalous GVD while the beam 2 experiences normal GVD. Figures 6 and 7 show the results using the same parameter values as in case (b) and should be compared with Figs. 4 and 5, respectively. The qualitative behavior is the same in both cases. In fact, Eqs. (28)–(30) are invariant under the interchange of the subscripts 1 and 2, showing the equivalence of the two cases. Thus the results of Figs. 4 and 5 also apply to case (c) if f_1 and f_2 as well as P_1 and P_2 are interchanged. Similarly, the results of Figs. 6 and 7 can apply to case (b).

Case (d): $\beta_1 < 0$, $\beta_2 < 0$. In this case both beams propagate in the anomalous-GVD region of the fiber. This case is interesting since each beam can develop modulation instability even in the absence of the XPM coupling between the two. Figures 8 and 9 show the gain in the case of induced and spontaneous modulation instabilities, respectively. These figures should be compared with Figs. 2 and 3 drawn for the case in which both beams experience normal GVD. The gain is larger by a factor of about 4 in the case of anomalous dispersion. In fact, the gain is larger by a factor of about 3 when $P_1 = P_2$ from that expected in the absence of the second beam [see Eq. (26)]. This can be seen in Fig. 9 where the limit $P_2 = 0$ corresponds to the conventional single-beam modulation instability. The presence of the second beam facilitates the development of modulation on both beams. This is not surprising if we note that both SPM and XPM contribute to the nonlinear phase shift that is converted to intensity modulation in the presence of GVD.

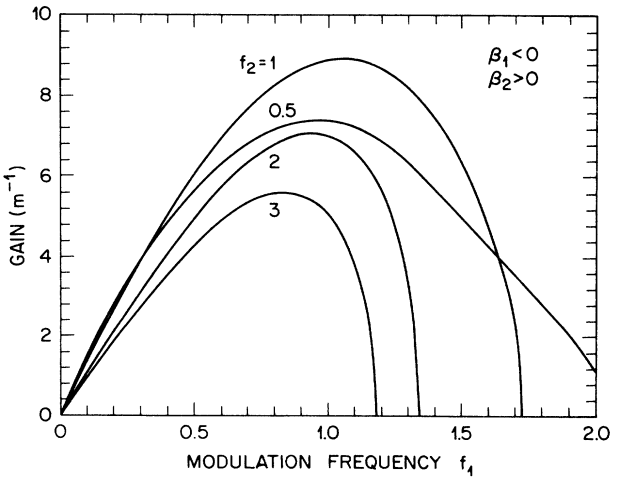

FIG. 6. Same as Fig. 2 except that beam 1 experiences anomalous GVD ($\beta_1 < 0$) while beam 2 experiences normal GVD ($\beta_2 > 0$).

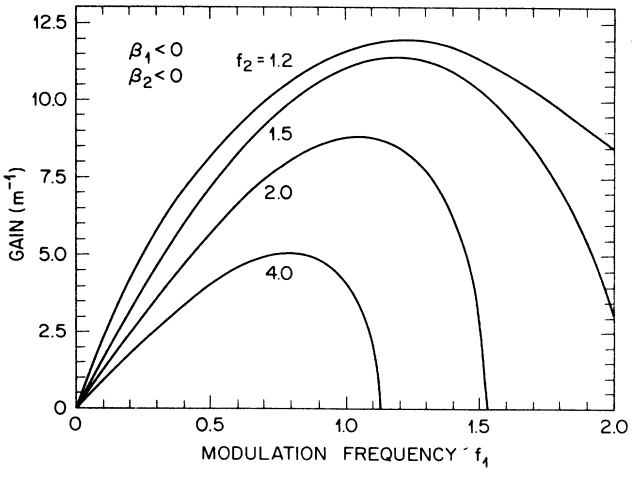

FIG. 8. Same as Fig. 2 except that both beams experience anomalous GVD ($\beta_1 < 0$, $\beta_2 < 0$).

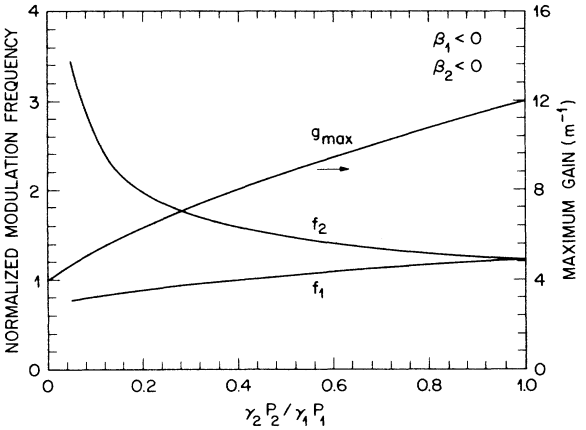

FIG. 9. Same as Fig. 3 except that both beams experience anomalous GVD ($\beta_1 < 0, \beta_2 < 0$).

V. DISCUSSION AND CONCLUSION

The results of this paper show that propagation of an optical beam inside the single-mode fibers is influenced substantially by the presence of a second copropagating beam. The wavelength difference between the two beams is immaterial and can be quite large. The coupling between the two beams results from XPM and has its origin in the intensity dependence of the refractive index. Even though such a coupling affects only the phase of cw beams, it can lead to dramatic changes in the stability of the cw beams in the presence of GVD. The most notable change occurs when both beams propagate in the normal-GVD regime of the optical fiber. Even though each beam is expected to propagate stably by itself, the two beams develop temporal modulations (self-pulsing) when propagated simultaneously. The modulation instability in this case is solely due to XPM. In other cases in which one or both beams propagate in the anomalous-GVD regime XPM affects significantly the characteristics of modulation instability. In particular, it enhances the gain experienced by the modulations imposed on the cw beam. As a result, the modulation-instability side bands grow at a faster rate and can be observed for shorter fiber lengths.

The experimental observation of the XPM-induced modulation instability would require the use of pulsed beams rather than cw beams to avoid the competing nonlinear effects such as stimulated Brillouin scattering. The analysis of this paper can still be applied as long as the pulse width is much larger than the modulation period or $\Omega_j T_j \gg 1$, where $j = 1$ or 2, and T_1 and T_2 are the pulse widths for the two beams. Since $\Omega_j / 2\pi \gtrsim 2$ THz in most cases of practical interest, this condition is easily satisfied for $T_j > 10$ ps. A second limitation on the pulse width results from the group-velocity mismatch between the two pulses. Because of their different speeds, the two pulses separate from each other after a distance $z \sim L_W$, where L_W is the so-called walk-off length defined as $L_W = T_j / |v_g^{-1} - v_{g2}^{-1}|$. The walk-off length depends not only on the pulse width but also on the wavelength separation between the two pulses. For the 10-ps pulses and 10-nm wavelength separation in the visible region, $L_W \simeq 2$ m, but can reduce by an order of magnitude for a wavelength separation ~ 100 nm. The XPM interaction occurs as long as the two pulses physically overlap. Thus, L_W should be large enough for the modulation to build up from the noise. The results shown in Figs. 2–9 show that small-signal gain $g = 5-10$ m^{-1} is expected for pulses with peak powers ~ 100 W. If we use $gL_W \simeq 16$ as a rough criterion for the significant growth of modulation instability,[14] $L_W \sim 2$ m is needed. This can be easily achieved for pulses as short as 10 ps if the wavelength separation is about 10 nm.

This paper has considered the case in which both beams are incident externally on the fiber. An interesting situation occurs when only one beam is incident and the second beam is internally generated through stimulated Raman scattering. In fact, the first observation of XPM-induced modulation instability[34] in the normal-dispersion regime has been made in this configuration. In this experiment, the 25-ps pulses at 532 nm, obtained from a mode-locked Nd:YAG laser, were propagated through a fiber whose length was varied in the range 0.5–10 m. The peak power of pump pulses was large enough to exceed the Raman threshold and to generate a Stokes wave at a wavelength of about 544 nm. The spectra of both the pump and the Stokes pulses developed modulation side bands at the fiber output, a clear signature of modulation instability. Furthermore, the shift of the modulation side bands from the center wavelength was in agreement with the theoretical prediction as Sec. III. A detailed comparison is not feasible because of the complications resulting from pump depletion and the Raman gain that leads to power changes for both beams.

Recently modulation instability has also been observed for the case in which both beams are incident externally.[35] In this experiment, a strong 500-ps pulse at 1.06 μm was copropagated with a weak 100-ps pulse at 1.32 μm in a fiber with a zero-dispersion wavelength near 1.27 μm. This configuration corresponds to case (b) of Sec. IV. the weak 1.32-μm pulse developed modulation side bands separated from the center frequency by 0.29 THz. The autocorrelation measurements confirmed the 3.5-ps modulation superimposed on the 100-ps pulse as a result of modulation instability.

This paper considered the XPM interaction between two beams of different wavelengths. The XPM interaction can also occur when two spatially separated beams in a nonlinear directional coupler are coupled through evanescent waves.[39] An example is provided by a dual-core fiber that can act as an ultrafast all-optical switch.[40] Modulation instability can occur in such nonlinear couplers and may influence their characteristics. Another interesting case corresponds to the XPM interaction between the two polarization components of the same beam in a birefringent fiber. The XPM-induced modulation instability leads to the temporal modulation of both polarization components.[41] Similar to the case discussed here, such instabilities can occur even in the normal-GVD regime of the fiber. The results of this paper show that optical beams at different wavelengths do not propa-

gate independently in the presence of fiber nonlinearities. This can have important ramifications when optical fibers are used as a nonlinear coupler or switch. On the practical side, the XPM-induced interaction may be useful for generating ultrashort (< 100 fs) pulses in the visible region.

ACKNOWLEDGMENT

The research at City College of New York is supported in part by Hamamatsu Photonics K.K.

---

*Present Address: Institute of Optics, University of Rochester, Rochester, NY 14627.

[1]G. B. Whitham, Proc R. Soc. London **283**, 238 (1965); J. Fluid Mech. **27**, 399 (1967).

[2]T. B. Benjamin and J. E. Feir, J. Fluid Mech. **27**, 417 (1967).

[3]V. I. Bespalov and V. I. Talanov, Pisma Zh. Eksp. Teor. Fiz. **3**, 471 (1966) [JETP Lett. **3**, 307 (1966)].

[4]V. I. Karpman, Pisma Zh. Eksp. Teor. Fiz. **6**, 829 (1967) [JETP Lett. **6**, 227 (1967)]; V. I. Karpman and E. M. Krushkal, Zh. Eksp. Teor. Fiz **55**, 530 (1968) [Sov. Phys.—JETP **28**, 277 (1969)].

[5]L. A. Ostrovskii, Zh. Eksp. Teor. Fiz. **51**, 1189 (1966). [Sov. Phys.—JETP **24**, 797 (1967)].

[6]T. Tainuti and H. Washimi, Phys. Rev. Lett. **21**, 209 (1968).

[7]C. K. W. Tam, Phys. Fluids **12**, 1028 (1969).

[8]A. Hasegawa, Phys. Rev. Lett. **24**, 1165 (1970); Phys. Fluids **15**, 870 (1971).

[9]A. Hasegawa and W. F. Brinkman, IEEE J. Quantum Electron. **QE-16**, 694 (1980).

[10]A. Hasegawa, Opt. Lett. **9**, 288 (1984).

[11]D. Anderson and M. Lisak, Opt. Lett **9**, 468 (1984).

[12]B. Hermansson and D. Yevick, Opt. Commun. **52**, 99 (1984).

[13]N. N. Akhmedieva, V. M. Eleonskii, and N. E. Kulagin, Zh. Eksp. Teor. Fiz **89**, 1542 (1985) [Sov. Phys.—JETP **62**, 894 (1985)].

[14]K. Tai, A. Hasegawa, and A. Tomita, Phys. Rev. Lett. **56**, 135 (1986).

[15]K. Tai, A. Tomita, J. L. Jewell, and A. Hasegawa, Appl. Phys. Lett. **49**, 236 (1986).

[16]P. K. Shukla and J. J. Rasmussen, Opt. **11**, 171 (1986).

[17]K. Tajima, J. Lightwave Technol. **LT-4**, 900 (1986).

[18]N. C. Kothari, Opt. Commun. **62**, 247 (1987).

[19]M. J. Potasek, Opt. Lett. **12**, 921 (1987).

[20]M. J. Potasek and G. P. Agrawal, Phys. Rev. A **36**, 3862 (1987).

[21]V. A. Vysloukh and N. A. Sukhotskova, Kvant. Elektron, (Moscow) **14**, 2371 (1987) [Sov. J. Quantum Electron. **17**, 1509 (1987)].

[22]M. N. Islam, S. P. Dijaili, and J. P. Gordon, Opt. Lett. **13**, 518 (1988).

[23]G. P. Agrawal, *Nonlinear Fiber Optics* (Academic, Boston, 1989), Chap. 5.

[24]G. P. Agrawal, Phys. Rev. Lett. **59**, 880 (1987).

[25]R. R. Alfano, Q. X. Li, T. Jimbo, J. T. Manassah, and P. P. Ho, Opt. Lett. **11**, 626 (1986).

[26]M. N. Islam, L. F. Mollenauer, R. H. Stolen, J. R. Simpson, and H. T. Shang, Opt. Lett. **8**, 625 (1987).

[27]R. R. Alfano and P. P. Ho, IEEE J. Quantum Electron. **QE-24**, 351 (1988).

[28]D. Schadt and B. Jaskorzynska, J. Opt. Soc. Am. B **4**, 856 (1987); **5**, 2374 (1988).

[29]J. T. Manassah, Appl. Opt. **26**, 3747 (1987); **26**, 3750 (1987); Opt. Lett. **13**, 755 (1988).

[30]D. Schadt and B. Jaskorzynska, Electron. Lett. **23**, 1091 (1987); B. Jarskorzynska and D. Schadt, IEEE J. Quantum Electron. **QE-24**, 2117 (1988).

[31]P. L. Baldeck, R. R. Alfano, and G. P. Agrawal, Appl. Phys. Lett. **52**, 1939 (1988).

[32]S. Trillo, S. Wabnitz, E. M. Wright, and G. I. Stegeman, Opt. Lett. **13**, 871 (1988).

[33]G. P. Agrawal, P. L. Baldeck, and R. R. Alfano, Opt. Lett. **14**, 137 (1989).

[34]P. L. Baldeck, R. R. Alfano, and G. P. Agrawal, in *Ultrafast Phenomena VI,* edited by T. Yajima, K. Yushihara, C. B. Harris, and S. Shionoya (Springer-Verlag, Berlin, 1988), pp. 53–55.

[35]A. S. Gouveia-Neto, M. E. Faldon, A. S. B. Sombra, P. G. J. Wigley, and J. R. Taylor, Opt. Lett. **13**, 901 (1988).

[36]*Optical Instabilities,* edited by R. W. Boyd, M. G. Raymer, and L. M. Narducci (Cambridge University Press, London, 1986).

[37]*Instabilities and Chaos in Quantum Optics,* edited by F. T. Arecchi and R. G. Harrison (Springer-Verlag, Heidelberg, 1987).

[38]See, for example, the review paper by B. J. Ainslie and C. R. Day, J. Lightwave Technol. **LT-4**, 967 (1986).

[39]Y. Siberberg and G. I. Stegeman, Appl. Phys. Lett. **50**, 801 (1987).

[40]S. R. Friberg, Y. Silberberg, M. K. Oliver, M. J. Andrejco, M. A. Saffi, and P. W. Smith Appl. Phys. Lett. **51**, 1135 (1987).

[41]S. Wabnitz, Phys. Rev. A **38**, 2018 (1988).